

Article

Omnibus Modeling of *Listeria monocytogenes* Growth Rates at Low Temperatures

Vincenzo Pennone ¹, Ursula Gonzales-Barron ², Kevin Hunt ³, Vasco Cadavez ², Olivia McAuliffe ¹
and Francis Butler ^{3,*}

¹ Teagasc Food Research Centre, Moorepark, Fermoy, P61 C996 Co Cork, Ireland; vincenzopennone@hotmail.it (V.P.); Olivia.McAuliffe@teagasc.ie (O.M.)

² Centro de Investigação de Montanha (CIMO), Instituto Politécnico de Bragança, Campus de Santa Apolónia, 5300-253 Bragança, Portugal; ubarron@ipb.pt (U.G.-B.); vcadavez@ipb.pt (V.C.)

³ UCD School of Biosystems and Food Engineering, University College Dublin, Belfield, Dublin 4, Ireland; kevin.hunt@ucd.ie

* Correspondence: f.butler@ucd.ie

Abstract: *Listeria monocytogenes* is a pathogen of considerable public health importance with a high case fatality. *L. monocytogenes* can grow at refrigeration temperatures and is of particular concern for ready-to-eat foods that require refrigeration. There is substantial interest in conducting and modeling shelf-life studies on *L. monocytogenes*, especially relating to storage temperature. Growth model parameters are generally estimated from constant-temperature growth experiments. Traditionally, first-order and second-order modeling (or primary and secondary) of growth data has been done sequentially. However, omnibus modeling, using a mixed-effects nonlinear regression approach, can model a full dataset covering all experimental conditions in one step. This study compared omnibus modeling to conventional sequential first-order/second-order modeling of growth data for five strains of *L. monocytogenes*. The omnibus model coupled a Huang primary model for growth with secondary models for growth rate and lag phase duration. First-order modeling indicated there were small significant differences in growth rate depending on the strain at all temperatures. Omnibus modeling indicated smaller differences. Overall, there was broad agreement between the estimates of growth rate obtained by the first-order and omnibus modeling. Through an appropriate choice of fixed and random effects incorporated in the omnibus model, potential errors in a dataset from one environmental condition can be identified and explored.

Keywords: omnibus modeling; *Listeria monocytogenes*; predictive microbiology; growth models; Huang model



Citation: Pennone, V.; Gonzales-Barron, U.; Hunt, K.; Cadavez, V.; McAuliffe, O.; Butler, F. Omnibus Modeling of *Listeria monocytogenes* Growth Rates at Low Temperatures. *Foods* **2021**, *10*, 1099. <https://doi.org/10.3390/foods10051099>

Academic Editors: Arun K. Bhunia and Robert L. Buchanan

Received: 23 February 2021

Accepted: 12 May 2021

Published: 15 May 2021

Publisher's Note: MDPI stays neutral with regard to jurisdictional claims in published maps and institutional affiliations.



Copyright: © 2021 by the authors. Licensee MDPI, Basel, Switzerland. This article is an open access article distributed under the terms and conditions of the Creative Commons Attribution (CC BY) license (<https://creativecommons.org/licenses/by/4.0/>).

1. Introduction

Listeria monocytogenes is a facultatively anaerobic Gram-positive bacterium which is pathogenic for humans and is of considerable public health importance. Within the European Union, EFSA [1] reported 2549 human cases of listeriosis (0.47 cases per 100,000 population) in 2018 with a statistically significant increasing trend from 2009–2018. While the number of cases per 100,000 population was lower than for other food-borne pathogens, EFSA reported that the case fatality was high (15.6%) and concluded that listeriosis is one of the most serious food-borne diseases [1]. *L. monocytogenes* is psychrotrophic; thus, it can grow at refrigeration temperatures. For this reason, *L. monocytogenes* is of particular concern for ready-to-eat (RTE) foods that require refrigerated storage. There has been substantial activity within the European Union and elsewhere to provide guidance on how to conduct laboratory shelf-life studies on *L. monocytogenes* in RTE foods to assure product safety and to conform to regulatory requirements. Recently, several guidance documents have emerged outlining the conduct of challenge studies relating to *L. monocytogenes* in RTE foods. The EC/DG SANCO guidance [2] documents a decision tree approach for the steps

of shelf-life studies in order to investigate the growth of *L. monocytogenes* in the product. More recently, an EURL Lm Technical Guidance Document [3] details challenge tests and durability studies related to the growth of *L. monocytogenes* in RTE foods. In addition, an ISO standard—ISO 20976-1 [4]—provides further guidance on the conduct of challenge tests for any microorganism of concern. Other guidance documents are also available [5,6].

Growth kinetic parameters are generally estimated from constant-temperature growth experiments carried out during challenge testing using a primary growth model, where microbial counts are modeled as a function of time. Many primary models exist including the commonly used modified Gompertz model [7], the Baranyi model [8], the Buchanan model [9], and the Huang model [10]. Where appropriate, secondary models may also be applied to describe the effects of environmental factors such as temperature, water activity, and pH on the primary model parameters such as growth rate or lag time. A classic example of a secondary model is the Ratkowsky square-root model [11], which describes how growth rate varies with temperature.

Traditionally, first-order and second-order modeling has been done sequentially. Typically, a primary model is first fitted to a series of datasets on growth over time, carried out at constant temperature. The estimated parameters derived from the primary models are then subsequently used to fit to a secondary model describing, for example, the effect of temperature on growth rate. However, using a mixed-effects nonlinear regression approach, a full dataset covering all experimental conditions can be modeled at once. This type of modeling that fits the primary and secondary models at the same time is known as omnibus or global modeling [12,13]. Omnibus modeling is more advantageous than the classical two-step modeling because there is no loss of information related to the uncertainty of the kinetic parameters of the primary model, and random effects can accommodate the variability in parameters that cannot be explained by the environmental conditions [14]. The objective of this work was to compare omnibus modeling to a conventional sequential first-order/second-order modeling for growth studies carried out between 4 and 12 °C for five strains of *L. monocytogenes*. Previous studies demonstrated the strain-to-strain variability in growth rate for *L. monocytogenes* [15,16]. There is also evidence that the variability is higher at refrigerated temperatures of 4–7 °C [15,17,18].

2. Materials and Methods

2.1. *Listeria monocytogenes* Strains

Five *L. monocytogenes* strains were used for this study. The strains were chosen to be representative of ongoing challenge studies of *L. monocytogenes* in a range of dairy and seafood matrices. Three strains, 12MOB079LM (dairy source), 12MOB099LM (seafood), and 12MOB104LM (seafood), were selected from the EURL Lm strain collection [3]. Isolate 954 (dairy) was from the Teagasc *L. monocytogenes* collection (Teagasc, Moorepark, Co Cork, Ireland) and isolate 1513COB874 (seafood) was obtained from National University Ireland, Galway. The isolates were stored at −20 °C in 20% glycerol until required.

2.2. Growth Determination

As required, each strain was plated on Agar *Listeria* according to Ottaviani and Agosti (OAA—Ottaviani Agosti ready-to-use agar plates, BioMérieux, Marcy l’Etoile, France), and the plates were incubated for 48 h at 37 °C. One single colony of each isolate was resuspended in 10 mL of Brain Heart Infusion broth (BHI, Merck, Ireland) and incubated at 37 °C for 18 h. Serial dilutions were performed with saline solution (NaCl 0.85%), and 100 µL of the final dilution was added to 10 mL of BHI broth, to ensure an inoculum concentration of nominally 1000 CFU/mL. The inoculum concentration was assessed by plate counting. Each BHI tube was incubated at 4.5 °C, 7.8 °C, or 12.0 °C. At each timepoint, serial dilutions were prepared, and 10 µL of each dilution was pipetted onto BHI agar. The plates were incubated at 37 °C for 18 h, and the colonies were counted for quantification. Each isolate was cultured in three biological replicates (starting each time with a new

inoculum from the original isolate) for each temperature condition, and each dilution was plated in duplicate.

2.3. First-Order Growth Rate Modeling

To determine growth rate, the growth of *L. monocytogenes* at constant temperature was modeled using a three-phase Huang model [10]. This model is an adaption of a standard logistic growth curve to include an initial lag phase. The model uses four parameters to predict the CFU population at time t (Nt): the lag time (lag), unit h, the initial population (N_0), the maximum growth rate (μ_{\max}), unit h^{-1} , and the maximum population size (N_{\max}). α is the lag phase transition coefficient. Huang [10] reported that the value of α was not affected by bacteria type or temperature and determined it to be approximately 4, which is the value used in this study.

$$\ln(Nt) = \ln(N_0) + \ln(N_{\max}) - e^{\ln(N_0)} + \left(e^{\ln(N_{\max})} - e^{\ln(N_0)} \right) e^{-\mu_{\max} * \beta(t)}. \quad (1)$$

$$\beta(t) = t + \frac{1}{\alpha} \ln \left(1 + \frac{e^{-\alpha * (t - \text{lag})}}{e^{\alpha * \text{lag}}} \right). \quad (2)$$

The model (Equation (1)) was fitted separately for each strain, temperature condition, and biological replicate using the package *nlme* in the statistical programming language R (R Core Group, [19]). For a small number of experiments at 7.8 °C, full stationary growth conditions were not achieved. In these cases, a simplified two-phase version [10] was fitted instead. This model reduces the parameters of interest to a lag phase (lag) and an exponential growth rate (μ_{\max}), units h and h^{-1} , respectively (Equation (3)). For the reduced model, Huang [10] assigned a value of 25 to α , which is also the value used in this study.

$$\ln Nt = \ln N_0 + \mu_{\max} * \left(t + \frac{1}{\alpha} * \ln \left(\frac{1 + e^{-\alpha(t - \text{lag})}}{1 + e^{\alpha * \text{lag}}} \right) \right). \quad (3)$$

Differences between the growth rate parameter for each strain were compared using one-way analysis of variance at each temperature condition. If significance was determined, pairwise comparisons were made using a Tukey test. ANOVA assumptions were tested by residual analysis. Normality of residuals was assessed with a Shapiro–Wilk test, and homogeneity of variances was determined by a Levene test. All statistical analyses were carried out in R version 3.6.3 [19], using R Studio version 1.0.136.

2.4. Omnibus Modeling of Growth Curves

The growth of each of the *L. monocytogenes* strains was described by an omnibus model that coupled a primary model for growth to secondary models for growth rate and lag phase duration.

The omnibus model of the form,

$$Y_{ij} = Y_{0j} + Y_{\max j} - \ln \{ \exp(Y_{0j}) + (\exp(Y_{\max j}) - \exp(Y_{0j})) \times \exp(-\mu_{\max j} \times B_{ij}) \} + \varepsilon_{ij}, \quad (4)$$

$$B_{ij} = t_i + \frac{1}{\alpha} \ln \frac{1 + \exp(-\alpha \times (t_i - \lambda_j))}{1 + \exp(\alpha \times \lambda_j)}, \quad (5)$$

$$Y_{0j} = Y_0 + u_j, \quad (6)$$

$$\frac{1}{\sqrt{\lambda_j}} = \gamma_0 + \gamma_1 \text{Temp}_j^2, \quad (7)$$

$$\sqrt{\mu_{\max j}} = (\beta_0 + v_j) + \beta_1 \text{Temp}_j, \quad (8)$$

$$Y_{\max j} = Y_{\max} + w_j, \quad (9)$$

is essentially a multilevel model, and it was adjusted to each of the five *L. monocytogenes* strain datasets, as a nonlinear mixed-effects regression.

The primary model for growth chosen was the Huang full model [10] (Equation (4)), whereas the secondary models were simple data-driven polynomial models that were defined before omnibus modeling. The goodness of fit of the secondary models for the lag phase duration (Equation (6)) and maximum growth rate (Equation (7)) was assessed by simple graphs of normality of residuals, predicted values versus observations, and residuals versus fitted values. More complex secondary models could not be considered since the number of temperature levels was only three.

The microbial concentration ($\ln \text{CFU} \cdot \text{mL}^{-1}$) of *L. monocytogenes* measured at time i when subjected to the environmental condition j is represented by Y_{ij} . Y_{0j} is the initial microbial concentration ($\ln \text{CFU} \cdot \text{mL}^{-1}$) in a given environmental condition j . In this case, the environmental condition j is defined by the temperature of incubation $Temp$ as a class variable. Since inoculum size was not exactly the same for every run, the mean initial microbial concentration Y_0 was set to take in random effects u_j that varied from condition to condition. Y_{\max} denotes the maximum microbial concentration ($\ln \text{CFU}/\text{mL}$), which is also affected by random deviations w_j due to condition j . The microbial growth rate ($\ln \text{CFU} \cdot \text{h}^{-1}$) and lag phase duration (h) of *L. monocytogenes*, belonging to the environmental condition j , are represented by $\mu_{\max j}$ and λ_j , respectively. Nonetheless, to describe these two kinetic parameters as a function of temperature ($Temp$), they underwent transformations that were in advance proven to reduce heteroscedasticity. A square-root transformation was used for the microbial growth ($\sqrt{(\mu_{\max j})}$), whereas a reciprocal square-root transformation was applied to the lag phase duration ($1/\sqrt{(\lambda_j)}$). γ_1 is the quadratic effect of temperature on $1/\sqrt{(\lambda_j)}$, whereas γ_0 is the intercept of this function. Residual or unexplained variability in $\sqrt{(\mu_{\max j})}$ was extracted by the random effects v_j as realizations of the environmental condition j . Unlike the expression for the transformed maximum growth rate, which presented a stochastic component to account for the unexplained variability, the transformed lag phase duration ($1/\sqrt{(\lambda_j)}$) could be estimated only by the fixed effects γ_0 of the intercept and γ_1 of the temperature. No residual variability term was added to $1/\sqrt{(\lambda_j)}$ since the standard deviation of the random effects was consistently shown to be nonsignificant in the five omnibus models (i.e., belonging to the five *L. monocytogenes* strains). The random effects u_j , v_j , and w_j were assumed to be correlated following a multi-normal distribution with

mean zero and variance matrix $\begin{vmatrix} s_u^2 & & \\ S_u S_v & s_v^2 & \\ S_u S_w & S_v S_w & s_w^2 \end{vmatrix}$. Coefficients of correlations between random effects were then calculated. The residuals ε_{ij} were assumed to follow a normal distribution with mean zero and standard deviation s . In addition to the parameter estimates and the variance components, the correlation coefficients between observations and fitted values ($R_{obs-fit}$) and between fitted values and residuals ($R_{fit-residuals}$) were calculated for every omnibus model, for assessment of goodness of fit.

2.5. Omnibus Modeling of the Growth of *L. monocytogenes* for the Five Strains

An overarching omnibus model was used to describe the growth of the five separate *L. monocytogenes* strains.

$$Y_{is(j)} = Y_{0s(j)} + Y_{\max s(j)} - \ln \left\{ \exp \left(Y_{0s(j)} \right) + \left(\exp \left(Y_{\max s(j)} \right) - \exp \left(Y_{0s(j)} \right) \right) \times \exp \left(-\mu_{\max s(j)} \times B_{is(j)} \right) \right\} + \varepsilon_{is(j)}. \quad (10)$$

$$B_{is(j)} = t_i + \frac{1}{4} \ln \frac{1 + \exp \left(-4 \times \left(t_i - \lambda_{s(j)} \right) \right)}{1 + \exp \left(4 \times \lambda_{s(j)} \right)}. \quad (11)$$

$$Y_{0s(j)} = Y_0 + u_s + u_{s(j)}. \quad (12)$$

$$\frac{1}{\sqrt{\lambda_{s(j)}}} = (\gamma_0 + v_s + v_{s(j)}) + \gamma_1 Temp_j^2. \tag{13}$$

$$\sqrt{\mu_{\max s(j)}} = (\beta_0 + w_s + w_{s(j)}) + \beta_1 Temp_j. \tag{14}$$

$$Y_{\max s(j)} = Y_{\max} + z_s + z_{s(j)}. \tag{15}$$

This general omnibus model presented the same fixed-effects architecture as the strain-specific omnibus model (Equation (4)), yet with a different clustering structure that nested environmental conditions j within strain s . Thus, Equation (9) was fitted to the entire dataset, whereby the observations $Y_{is(j)}$ were now defined as the microbial concentration (ln CFU·mL⁻¹) of *L. monocytogenes* strain s measured at time i when subjected to the environmental condition j . The variables $Y_{0 s(j)}$, $1/\sqrt{\lambda_{s(j)}}$, $\sqrt{\mu_{\max s(j)}}$, and $Y_{\max s(j)}$ were allowed to take in the nested random shifts $u_s + u_{s(j)}$, $v_s + v_{s(j)}$, $w_s + w_{s(j)}$, and $z_s + z_{s(j)}$, respectively, as realizations of the strain s and the environmental condition j nested in strain s . With this error structure arrangement, it is possible to separate the residual variability in $Y_{is(j)}$ due to the experimental condition from the actual inter-strain variability. The random effects u_s , v_s , w_s , and z_s were assumed to be correlated and distributed as a multi-normal distribution with mean zero and the following covariance matrix:

$$\begin{vmatrix} s_{u_s}^2 & & & \\ S_{u_s S_{v_s}} & s_{v_s}^2 & & \\ S_{u_s S_{w_s}} & S_{v_s S_{w_s}} & s_{w_s}^2 & \\ S_{u_s S_{z_s}} & S_{v_s S_{z_s}} & S_{w_s S_{z_s}} & s_{z_s}^2 \end{vmatrix} \tag{16}$$

Likewise, the nested random effects $u_{s(j)}$, $v_{s(j)}$, $w_{s(j)}$, and $z_{s(j)}$ were assumed to be correlated and normally distributed with mean zero and the following covariance matrix:

$$\begin{vmatrix} s_{u_{s(j)}}^2 & & & & \\ S_{u_{s(j)} S_{v_{s(j)}}} & s_{v_{s(j)}}^2 & & & \\ S_{u_{s(j)} S_{w_{s(j)}}} & S_{v_{s(j)} S_{w_{s(j)}}} & s_{w_{s(j)}}^2 & & \\ S_{u_{s(j)} S_{z_{s(j)}}} & S_{v_{s(j)} S_{z_{s(j)}}} & S_{w_{s(j)} S_{z_{s(j)}}} & s_{z_{s(j)}}^2 & \end{vmatrix} \tag{17}$$

Coefficients of correlation between the nested random effects were calculated from the two matrices. The residuals $\epsilon_{is(j)}$ were assumed to follow a normal distribution with mean zero and standard deviation s .

2.6. Validation of the Omnibus Model

The overarching omnibus model shown in Equation (5) was fitted to the datasets from two of the temperatures, 4.5 and 12 °C, and used to predict the growth at 7.8 °C for model validation. The predictive capacity of the omnibus model was assessed by means of graphs of growth observations versus predicted growth curves for the five strains. In addition to the visual appraisal, the accuracy factor (Af) and bias factor (Bf) of the growth predictions were jointly calculated for all the growth curves [20]. All the nonlinear mixed-effects regression models were fitted using the *nlme* function from the *nlme* package [21] implemented in R Studio version 1.0.136 with R version 3.6.3 [19].

3. Results

3.1. Growth Curves

Figure 1 shows the representative growth curves for two of the strains at the three experimental temperatures. Superimposed on the experimental data points are the three-phase Huang model predictions. A period of exponential growth was observed in all strains at the three temperatures. As expected, as temperature increased, the lag time became shorter and the growth rate during the exponential phase became higher. For a small number of experiments at 7.8 °C, full stationary growth conditions were not achieved.

However, an estimate of the maximum concentration was normally possible from the models.

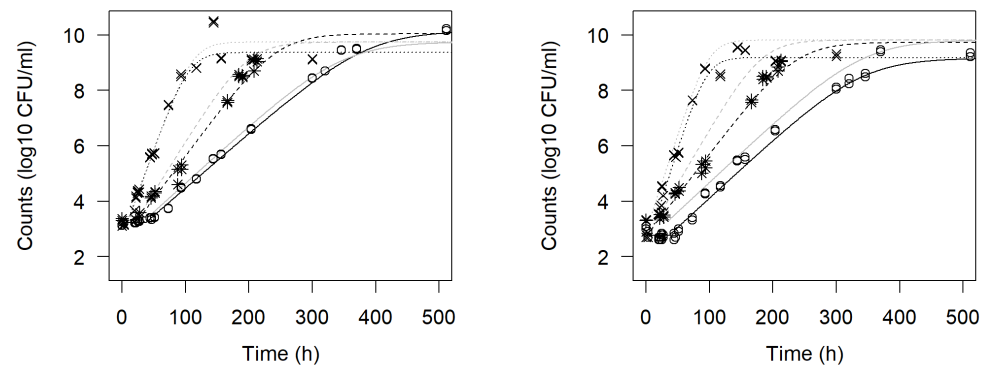


Figure 1. Representative experimental growth curves (one replicate) for *L. monocytogenes* strains 12MOB079LM (left) and 12MOB099LM (right) at the three measured temperatures (○ 4.5 °C, * 7.8 °C, × 12 °C) together with Huang model predictions derived from first-order modeling (darker lines) and omnibus modeling (lighter lines).

3.2. First-Order Growth Rate Modeling

Table 1 summarizes the growth rate parameter estimates for each strain at the recorded temperature. There were significant differences in growth rate depending on the strain at all three temperatures. At 4.5 °C, the mean growth rate varied between 0.0428 and 0.0476 h⁻¹. On the other hand, at 12 °C, the growth rate varied between 0.145 and 0.187 h⁻¹. The secondary effect of temperature on growth rate was compared among strains with multiple linear regression. Maximum growth rates were fitted with a square-root transformation, using the predictors temperature, strain, and their interaction. Figure 2 shows the growth rate values for each *L. monocytogenes* strain at each temperature. Multiple linear regression showed no significant difference between the intercept for any strain and only one significant ($p < 0.05$) difference in slope, for strain 1513COB874. Figure 2 also shows that, at 12 °C, there was more variability in the growth rate compared to the lower temperatures.

Table 1. Growth rate parameter estimates (STANDARD deviation of the three replicates in parenthesis) for each strain of *L. monocytogenes* and experimental temperature condition obtained by first-order modeling. Averages within a column followed by a common superscript letter are not significantly different ($p < 0.05$).

Strain	Growth Rate (h ⁻¹)		
	4.5 °C	7.8 °C	12.0 °C
954	0.043 ^b (0.00091)	0.068 ^b (0.00045)	0.15 ^{bc} (0.0027)
12MOB079LM	0.046 ^a (0.00038)	0.071 ^a (0.00069)	0.15 ^c (0.0040)
12MOB099LM	0.046 ^{ab} (0.00098)	0.069 ^{ab} (0.00071)	0.15 ^{bc} (0.0093)
12MOB104LM	0.048 ^a (0.0011)	0.068 ^b (0.00017)	0.16 ^b (0.0070)
1513COB874	0.045 ^{ab} (0.0022)	0.068 ^b (0.0016)	0.19 ^a (0.0034)

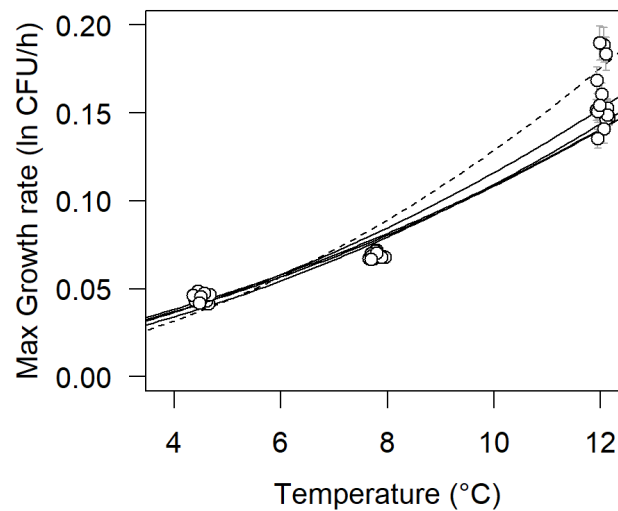


Figure 2. Maximum growth rate values for each *L. monocytogenes* strain (all replicates plotted) at each temperature (data points stretched at each temperature for clarity). Square-root transformed linear regressions are also plotted. The dotted line represents strain 1513COB874, whose transformed slope was the only significant difference observable ($p < 0.05$). A small random horizontal shift was added to the data points to improve their visibility.

3.3. Omnibus Modeling of Growth Curves

Tables 2–5 set out the omnibus model parameters for the five strains based on the complete dataset at the three temperatures. Estimates of the fixed-effect parameters, Y_0 (initial concentration (ln CFU·mL⁻¹)) were similar (~7.3 ln; 3.2 log₁₀) across the strains, with the exception of strain 12MOB104LM (6.7 ln; 2.9 log₁₀). Likewise, estimates of Y_{max} (final concentration (ln CFU·mL⁻¹)) were similar across the five strains (~21.4 ln; 9.3 log₁₀). Estimates of the predictors of $\sqrt{\mu_{max}}$, β_0 and β_1 , were also similar for the five strains, with the exception of strain 1513COB874. This outcome is consistent with what was reported from the first-order modeling and shown in Figure 2. The standard error reported for the estimates of the predictors of $\sqrt{\mu_{max}}$ were all low, indicating good consistency among replicates.

Table 2. Fixed- and random-effects estimates of the omnibus model describing the concentration (ln CFU/mL) of *L. monocytogenes* strain 954. Goodness-of-fit measures include coefficient of correlation of observed versus fitted values ($R_{obs-fit}$) and coefficient of correlation of fitted values versus residuals ($R_{fit-residuals}$).

Parameters	Mean	Standard Error	Pr > t	Other Analysis
Fixed effects				
Y_0 (ln CFU·mL ⁻¹)	7.280	0.205	<0.0001	
Y_{max} (ln CFU·mL ⁻¹)	21.48	0.475	<0.0001	
Predictor of $\sqrt{\mu_{max}}$				
β_0 (Intercept) (h ^{-0.5})	0.108	0.004	<0.0001	
β_1 (Temp) (h ^{-0.5} ·°C ⁻¹)	0.021	0.001	<0.0001	
Predictor of $1/\sqrt{\lambda}$				
γ_0 (Intercept) (h ^{-0.5})	0.145	0.009	<0.0001	$R_{obs-fit} = 0.997$
γ_1 (Temp ²) (h ^{-0.5} ·°C ⁻²)	0.0017	0.0003	<0.0001	$R_{fit-residuals} = 0.008$
Random effects (condition)				
		Correlation matrix		
s_u (Y_0) (ln CFU·mL ⁻¹)	0.302	s_u (Y_0)	s_w (Y_{max})	
s_v (β_0) (h ^{-0.5})	1.7×10^{-9}	0.725		
s_w (Y_{max}) (ln CFU·mL ⁻¹)	0.774	-0.582	-0.284	
s (residual)	0.507			

Table 3. Fixed- and random-effects estimates of the omnibus model describing the concentration (ln CFU/mL) of *L. monocytogenes* strain 12MOB079LM. Goodness-of-fit measures include coefficient of correlation of observed versus fitted values ($R_{\text{obs-fit}}$) and coefficient of correlation of fitted values versus residuals ($R_{\text{fit-residuals}}$).

Parameters	Mean	Standard Error	Pr > t	Other Analysis
Fixed effects				
Y_0 (ln CFU·mL ⁻¹)	7.318	0.107	<0.0001	
Y_{max} (ln CFU·mL ⁻¹)	21.86	0.135	<0.0001	
Predictor of $\sqrt{\mu_{\text{max}}}$				
β_0 (Intercept) (h ^{-0.5})	0.111	0.016	<0.0001	
β_1 (Temp) (h ^{-0.5} ·°C ⁻¹)	0.022	0.002	<0.0001	
Predictor of $1/\sqrt{\lambda}$				
γ_0 (Intercept) (h ^{-0.5})	0.135	0.010	<0.0001	$R_{\text{obs-fit}} = 0.995$
γ_1 (Temp ²) (h ^{-0.5} ·°C ⁻²)	0.001	0.0002	<0.0001	$R_{\text{fit-residuals}} = 0.002$
Random effects (condition)				
s_u (Y_0) (ln CFU·mL ⁻¹)	0.021	Correlation		
s_v (β_0) (h ^{-0.5})	0.009	s_u (Y_0)	s_w (Y_{max})	
s_w (Y_{max}) (ln CFU·mL ⁻¹)	3.2×10^{-7}	0.177		
s (residual)	0.572	0.006	0.030	

Table 4. Fixed- and random-effects estimates of the omnibus model describing the concentration (ln CFU/mL) of *L. monocytogenes* strain 12MOB099LM. Goodness-of-fit measures include coefficient of correlation of observed versus fitted values ($R_{\text{obs-fit}}$) and coefficient of correlation of fitted values versus residuals ($R_{\text{fit-residuals}}$).

Parameters	Mean	Standard Error	Pr > t	Other Analysis
Fixed effects				
Y_0 (ln CFU·mL ⁻¹)	7.420	0.170	<0.0001	
Y_{max} (ln CFU·mL ⁻¹)	21.09	0.208	<0.0001	
Predictor of $\sqrt{\mu_{\text{max}}}$				
β_0 (Intercept) (h ^{-0.5})	0.101	0.012	<0.0001	
β_1 (Temp) (h ^{-0.5} ·°C ⁻¹)	0.023	0.001	<0.0001	
Predictor of $1/\sqrt{\lambda}$				
γ_0 (Intercept) (h ^{-0.5})	0.129	0.009	<0.0001	$R_{\text{obs-fit}} = 0.996$
γ_1 (Temp ²) (h ^{-0.5} ·°C ⁻²)	0.001	0.0002	<0.0001	$R_{\text{fit-residuals}} = 0.001$
Random effects (condition)				
s_u (Y_0) (ln CFU·mL ⁻¹)	0.232	Correlation matrix		
s_v (β_0) (h ^{-0.5})	0.013	s_u (Y_0)	s_w (Y_{max})	
s_w (Y_{max}) (ln CFU·mL ⁻¹)	0.284	0.171		
s (residual)	0.508	-0.165	0.051	

With the exception of *L. monocytogenes* strain 12MOB079LM (Table 3), the between-condition variability in Y_0 (s_u), $\sqrt{\mu_{\text{max}}}$ (s_v), and Y_{max} (s_w) exhibited a similar trend for all strains. The variability in Y_{max} ranged between 0.284 and 0.848 ln CFU·mL⁻¹ (see s_w in Tables 2 and 4–6) and was consistently higher than the variability in Y_0 , which fell between 0.021 and 0.442 ln CFU·mL⁻¹ (see s_u in Tables 2 and 4–6). Since the omnibus models suggested that these two variabilities were not correlated ($r = -0.582, 0.006, -0.165, -0.091$, and -0.288 for all strains), it is reasonable to conclude that the inoculum concentration (related to Y_0) did not exert any effect on the maximum concentration reached in every experiment. Therefore, the higher variability observed in the maximum concentration may be linked to the absence of an observed stationary phase in some of the 7.8 °C data. This uncertainty increases the error in Y_{max} . In comparison to the variability in Y_0 (s_u) and Y_{max} (s_w), the variability in $\sqrt{\mu_{\text{max}}}$ was lower in all strains (s_v ranged from virtually zero to 0.017 in Tables 2–6), which indicates that temperature was able to explain most of the variability in $\sqrt{\mu_{\text{max}}}$, with low error associated with the estimation of $\sqrt{\mu_{\text{max}}}$. This fact

further indicates that the absence of a stationary phase in the 7.8 °C data did not affect the accurate estimation of $\sqrt{\mu_{\max}}$.

Table 5. Fixed- and random-effects estimates of the omnibus model describing the concentration (ln CFU/mL) of *L. monocytogenes* strain 12MOB104LM. Goodness-of-fit measures include coefficient of correlation of observed versus fitted values ($R_{\text{obs-fit}}$) and coefficient of correlation of fitted values versus residuals ($R_{\text{fit-residuals}}$).

Parameters	Mean	Standard Error	Pr > t	Other Analysis
Fixed effects				
Y_0 (ln CFU·mL ⁻¹)	6.709	0.241	<0.0001	
Y_{\max} (ln CFU·mL ⁻¹)	21.58	0.331	<0.0001	
Predictor of $\sqrt{\mu_{\max}}$				
β_0 (Intercept) (h ^{-0.5})	0.097	0.012	<0.0001	
β_1 (Temp) (h ^{-0.5} ·°C ⁻¹)	0.024	0.001	<0.0001	
Predictor of $1/\sqrt{\lambda}$				
γ_0 (Intercept) (h ^{-0.5})	0.129	0.011	<0.0001	$R_{\text{obs-fit}} = 0.996$
γ_1 (Temp ²) (h ^{-0.5} ·°C ⁻²)	0.002	0.0003	<0.0001	$R_{\text{fit-residuals}} = 0.013$
Random effects (condition)		Correlation matrix		
s_u (Y_0) (ln CFU·mL ⁻¹)	0.373	s_u (Y_0)	s_w (Y_{\max})	
s_v (β_0) (h ^{-0.5})	0.017	0.016		
s_w (Y_{\max}) (ln CFU·mL ⁻¹)	0.518	-0.091	0.031	
s (residual)	0.495			

Table 6. Fixed- and random-effects estimates of the omnibus model describing the concentration (ln CFU/mL) of *L. monocytogenes* strain 1513COB874. Goodness-of-fit measures include coefficient of correlation of observed versus fitted values ($R_{\text{obs-fit}}$) and coefficient of correlation of fitted values versus residuals ($R_{\text{fit-residuals}}$).

Parameters	Mean	Standard Error	Pr > t	Other Analysis
Fixed effects				
Y_0 (ln CFU·mL ⁻¹)	7.336	0.294	<0.0001	
Y_{\max} (ln CFU·mL ⁻¹)	21.05	0.518	<0.0001	
Predictor of $\sqrt{\mu_{\max}}$				
β_0 (Intercept) (h ^{-0.5})	0.089	0.007	<0.0001	
β_1 (Temp) (h ^{-0.5} ·°C ⁻¹)	0.027	0.001	<0.0001	
Predictor of $1/\sqrt{\lambda}$				
γ_0 (Intercept) (h ^{-0.5})	0.145	0.016	<0.0001	$R_{\text{obs-fit}} = 0.993$
γ_1 (Temp ²) (h ^{-0.5} ·°C ⁻²)	0.001	0.0003	<0.0001	$R_{\text{fit-residuals}} = -0.003$
Random effects (condition)		Correlation matrix		
s_u (Y_0) (ln CFU·mL ⁻¹)	0.442	s_u (Y_0)	s_w (Y_{\max})	
s_v (β_0) (h ^{-0.5})	9.9×10^{-9}	0.689		
s_w (Y_{\max}) (ln CFU·mL ⁻¹)	0.848	-0.288	-0.225	
s (residual)	0.667			

3.4. Omnibus Modeling of the Growth of *L. monocytogenes* for the Five Strains

Table 7 sets out the parameters from the overarching omnibus model used to describe the growth of the five *L. monocytogenes* strains. With the error structure arrangement, set up in Equation (5), it is possible to separate the residual variability in $Y_{is(j)}$ due to the experimental condition from the actual inter-strain variability. The values estimated for random effects due to strain, ranging between 8.5×10^{-8} for variability in lag phase and 5.7×10^{-5} for variability in maximum concentration (Table 7), clearly indicated that the variability among strains was negligible when assessed by omnibus modeling. In other words, strain did not appear to exert any effect on the microbial kinetic parameters.

However, most or nearly all variability in the kinetic parameters was as a result of the experimental conditions (temperature within strain). Again, the error in Y_{\max} (0.450 ln CFU·mL⁻¹) was slightly higher than the error in Y_0 (0.305 ln CFU·mL⁻¹) for the same reasons explained in the previous section. The overarching omnibus model confirmed

that the between-condition error associated with the estimation of $1/\sqrt{\lambda}$ was negligible ($s_{v\ s(j)} = 8.2 \times 10^{-8}$), while the error in estimating $\sqrt{\mu_{\max}}$ was also low ($s_{w\ s(j)} = 0.017$; Table 7). This demonstrates both (i) that the linear predictors of $1/\sqrt{\lambda}$ and $\sqrt{\mu_{\max}}$ defined in Equation (5) are adequate for describing the data and (ii) that the experiments were undertaken with good repeatability.

Using the estimated parameters in Table 7, it is possible to calculate maximum growth rates (μ_{\max}) at 4.5, 7.8, and 12.0 °C for the five strains (Table 8). There was very little difference in growth rates among strains at 4.5 °C. The variability among strains was largest at 12.0 °C, with strain 1513COB874 having the largest estimated strain rate. This is consistent with what was observed in Figure 2. In Figure 3, growth curves for the five strains of *L. monocytogenes* at 7.8 °C as predicted by the overarching omnibus model are superimposed on the count observations using the 7.8 °C data as a separate validation dataset. Agreement between the experimental data and predicted growth curves was very good in all cases (pooled Af = 1.173 and pooled Bf = 1.094).

Table 7. Fixed- and random-effects estimates of the overarching omnibus model describing the concentration (ln CFU·mL⁻¹) of five strains of *L. monocytogenes*. Goodness-of-fit measures include coefficient of correlation of observed versus fitted values ($R_{\text{obs-fit}}$) and coefficient of correlation of fitted values versus residuals ($R_{\text{fit-residuals}}$).

Parameters	Mean	Standard Error	Pr > t	Other Analysis
Fixed effects				
Y_0 (ln CFU·mL ⁻¹)	7.286	0.092	<0.0001	
Y_{\max} (ln CFU·mL ⁻¹)	21.69	0.150	<0.0001	
Predictor of $\sqrt{\mu_{\max}}$				
β_0 (Intercept) (h ^{-0.5})	0.098	0.013	<0.0001	
β_1 (Temp) (h ^{-0.5} ·°C ⁻¹)	0.024	0.001	<0.0001	
Predictor of $1/\sqrt{\lambda}$				
γ_0 (Intercept) (h ^{-0.5})	0.144	0.005	<0.0001	$R_{\text{obs-fit}} = 0.996$
γ_1 (Temp ²) (h ^{-0.5} ·°C ⁻²)	0.0013	0.0001	<0.0001	$R_{\text{fit-residuals}} = 0.006$
Nested random effects				
Strain <i>s</i>				
$s_{u\ s}$ (Y_0) (ln CFU·mL ⁻¹)	3.2×10^{-5}	Correlation matrix		$s_{z\ s}$ (Y_{\max})
$s_{v\ s}$ (γ_0) (h ^{-0.5})	8.5×10^{-8}	$s_{v\ s}$ (γ_0)	$s_{w\ s}$ (β_0)	
$s_{w\ s}$ (β_0) (h ^{-0.5})	2.8×10^{-6}	-0.148		
$s_{z\ s}$ (Y_{\max}) (ln CFU·mL ⁻¹)	5.7×10^{-5}	0.360	-0.226	0.543
		0.245	-0.003	
Condition <i>j</i> in Strain <i>s</i>				
$s_{u\ s(j)}$ (Y_0) (ln CFU·mL ⁻¹)	0.305	$s_{v\ s(j)}$ (γ_0)	$s_{w\ s(j)}$ (β_0)	$s_{z\ s(j)}$ (Y_{\max})
$s_{v\ s(j)}$ (γ_0) (h ^{-0.5})	8.2×10^{-8}	-0.763		
$s_{w\ s(j)}$ (β_0) (h ^{-0.5})	0.017	-0.385	0.719	
$s_{z\ s(j)}$ (Y_{\max}) (ln CFU·mL ⁻¹)	0.450	0.514	-0.511	-0.552
<i>s</i> (residual)	0.498			

Table 8. Mean and 95% confidence interval (CI) of the microbial growth rate (μ_{\max}) at 4.5, 7.8, and 12.0 °C for the five strains of *L. monocytogenes*, as estimated from the omnibus model.

Temperature (°C)	Strain	Mean μ_{\max} (h ⁻¹)	Low CI μ_{\max} (h ⁻¹)	High CI μ_{\max} (h ⁻¹)
4.5	954	0.0410	0.0364	0.0459
	12MOB079LM	0.0441	0.0304	0.0606
	12MOB099LM	0.0418	0.0321	0.0527
	12MOB104LM	0.0420	0.0324	0.0528
	1513COB874	0.0443	0.0377	0.0515
7.8	954	0.0738	0.0649	0.0835
	12MOB079LM	0.0799	0.0573	0.1068
	12MOB099LM	0.0787	0.0635	0.0951
	12MOB104LM	0.0807	0.0655	0.0973
	1513COB874	0.0897	0.0780	0.1025

Table 8. Cont.

Temperature (°C)	Strain	Mean μ_{\max} (h ⁻¹)	Low CI μ_{\max} (h ⁻¹)	High CI μ_{\max} (h ⁻¹)
12	954	0.1126	0.1049	0.1480
	12MOB079LM	0.1407	0.1017	0.1867
	12MOB099LM	0.1422	0.1180	0.1684
	12MOB104LM	0.1481	0.1234	0.1748
	1513COB874	0.1705	0.1490	0.1939

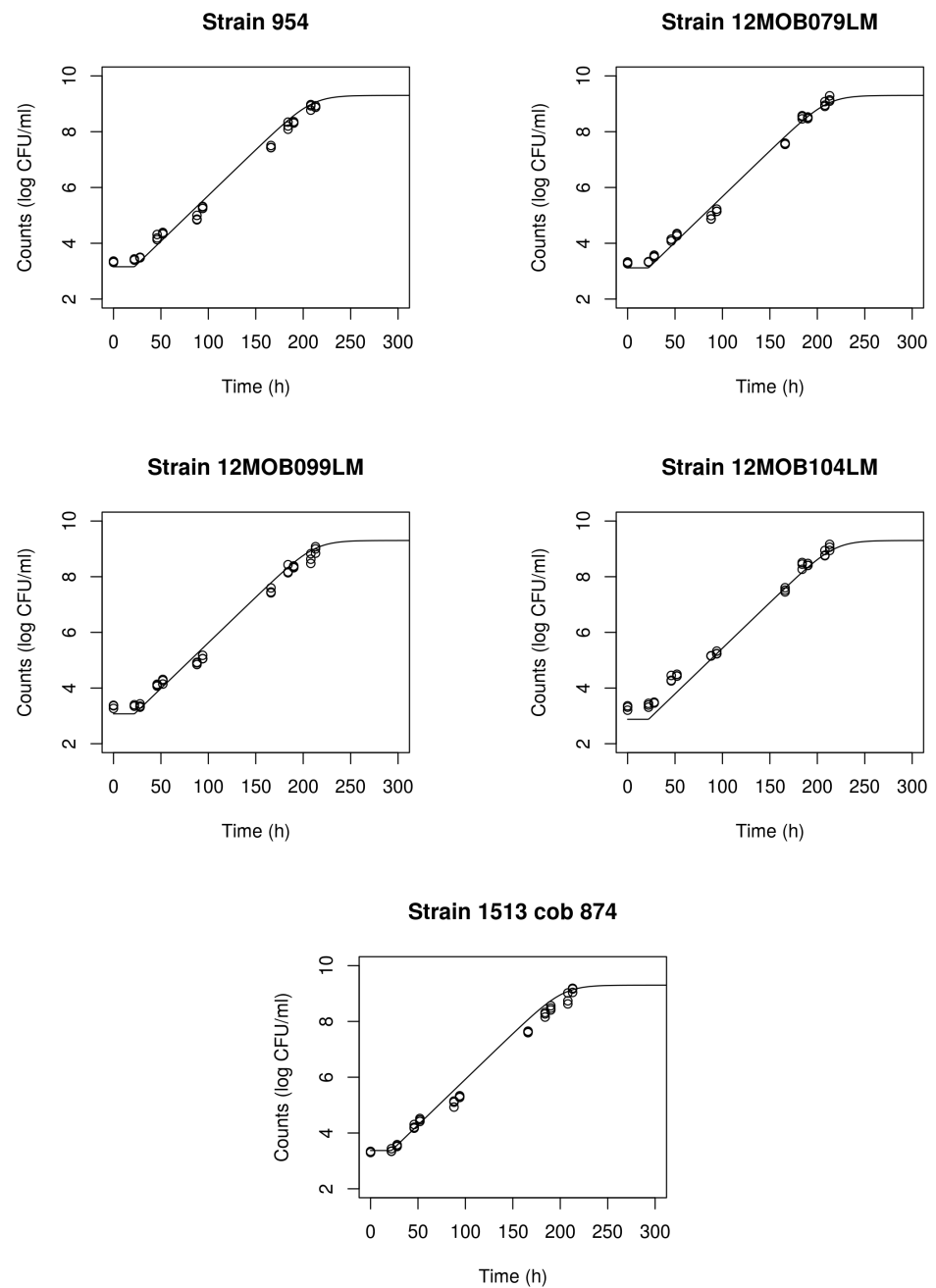


Figure 3. Growth curves for the five strains of *L. monocytogenes* stored at 7.8 °C, predicted by the overarching omnibus model against count observations using the separate validation dataset (pooled Af = 1.173 and pooled Bf = 1.094).

4. Discussion

Analysis of variance showed that there were some significant differences in growth rates among strains, which increased with temperature. At 4.5 °C, the largest difference was 11%, but this increased to 29% at 12 °C. To put this into perspective, the difference in reported growth rates [22] for the three the EURL *Lm* strains included in this study was 6% at 8 °C (Table 9). Moreover, Silva et al. [23] developed a web-based SHINY app which reports a meta-analysis estimate of growth rate for *L. monocytogenes* of 0.063 h⁻¹ with a 95% confidence interval between 0.0517 and 0.0755 h⁻¹ at 8 °C. The relatively large confidence intervals for the estimates of the growth rates in the present study (Table 8), determined from the omnibus modeling, indicate possibly small practical differences between strains for the growth rates estimated at a given temperature. Comparing Tables 1 and 8, there was broad agreement between the outcomes of the first-order and the omnibus modeling of growth rates across the five strains and three temperatures. The largest differences were at 7.8 °C, where the average differences between the two estimates was 17%. Again, these differences need to be judged within the context of the large confidence intervals for omnibus-derived growth rates already highlighted.

Table 9. Comparison of estimated maximum growth rates (h⁻¹) at 7.8 °C for the EURL *Lm* strains used in the study with published results.

Study	Current	EURL [18]	Shiny [21]	Combase [19]
Environment				
Temperature (°C)	7.8	8	8	8
pH	7.2	7	7	7
Aw	0.997	0.98	0.98	0.98
Strain				
12MOB079LM	0.080	0.093		
12MOB099LM	0.079	0.094		
12MOB104LM	0.081	0.089		
Model (op. density)			0.086	
Model (cell count)			0.063	0.071

Three of the strains were selected from the EURL *Lm* strain collection where reported growth rates have previously been reported [22]. In Table 9, the growth rate estimates from the omnibus modeling are compared to the EURL *Lm*-reported values [22] and to estimates derived from the publicly available COMBASE [24] predictions for *L. monocytogenes*, as well as predictions reported [23] using the web-based SHINY app. By necessity, there were small differences in the environmental conditions of temperature, pH, and Aw. The reported growth rates for the EURL *Lm* strains [22] were 10–19% higher than the values determined in the current study. However, the reported EURL *Lm* growth rates were determined by optical density measurements of cell growth against plate counts as used in the present study. Silva et al. [23] found using meta-analysis that growth rates determined by optical density measurements were normally higher than growth rates determined using conventional plating techniques. It is noteworthy that the two strains 12MOB079LM and 12MOB099LM are recommended for inclusion in low-temperature challenge tests [3] because of their high growth rates at low temperatures. This would partly explain why the current growth rate estimates for these two strains are higher than those predicted by the SHINY app [23], which represents a meta-analysis-derived average of many growth rate studies.

There have been relatively few published papers relating to the application of omnibus modeling to the growth of *L. monocytogenes*. To illustrate his new growth model, Huang [25] applied a primary model to the growth of *L. monocytogenes* in broth and frankfurters but did not employ omnibus modeling. Liu et al. [26] used omnibus modeling to describe the growth of *L. monocytogenes* in ready-to-eat braised beef. Other studies have also reported on the omnibus modeling approach [12,27,28]. The current work demonstrated a number

of advantages of the omnibus modeling approach. As the model is informed by all of the datasets obtained at different temperatures, there is no loss of information, and potential systematic errors in a dataset from one environmental condition can be identified and explored through an appropriate choice of fixed and random effects incorporated in the model. It is noteworthy that the first-order modeling predicted varying final-stage concentrations depending on temperature (Figure 1), whereas the omnibus modeling approach predicted an essentially similar final concentration irrespective of the temperature. Another benefit is the ability to interpolate across environmental conditions, such as temperature values, and to potentially compensate for incomplete datasets for one environmental condition. It is normal that, in comparison to the two-step approach, omnibus modeling produces wider confidence intervals for estimates of microbial concentrations or kinetic parameters, since, as there is no information loss and an error structure can be defined, the variance of the random effects extracted adds to the total variance associated to a prediction. Therefore, a higher number of significant random effects leads to wider confidence intervals.

In conclusion, the omnibus modeling approach represents a useful complementary approach to the classical methodology of sequential first-order and second-order modeling to further explore and gain insights from experimental growth data.

Author Contributions: Conceptualization, O.M., F.B., and U.G.-B.; methodology, O.M., V.P., U.G.-B., and V.C.; model development, U.G.-B., K.H., V.C., and F.B.; software, U.G.-B., V.C., and K.H.; validation, U.G.-B. and V.C.; formal analysis, U.G.-B., K.H., V.C., and F.B.; laboratory investigation, O.M. and V.P.; resources, O.M., F.B., and U.G.-B.; data curation, O.M., F.B., and V.P.; writing—original draft preparation, F.B. and K.H.; writing—review and editing, all.; visualization, K.H., U.G.-B., and V.C.; supervision, O.M. and F.B.; project administration, O.M. and F.B.; funding acquisition, O.M., F.B., and U.G.-B. All authors read and agreed to the published version of the manuscript.

Funding: This research was part funded by the Irish Department of Agriculture, Food, and Marine Research Funding Program, Project Reference 17/F/244, “Understanding *Listeria monocytogenes* growth in food”. U. Gonzales-Barron and V. Cadavez are grateful to the EU PRIMA program and the Portuguese Foundation for Science and Technology (FCT) for funding the ArtiSaneFood project (PRIMA/0001/2018) and to FCT for financial support through national funds FCT/MCTES to CIMO (UIDB/00690/2020). U. Gonzales-Barron acknowledges the national funding by FCT, P.I., through the Institutional Scientific Employment Program contract.

Data Availability Statement: The data presented in this study are available on request from the corresponding author.

Conflicts of Interest: The authors declare no conflict of interest. The funders had no role in the design of the study; in the collection, analyses, or interpretation of data; in the writing of the manuscript, or in the decision to publish the results.

References

1. EFSA. The European Union one health 2018 Zoonoses Report. *EFSA J.* **2019**, *17*, e05926.
2. EC/DG SANCO. *Commission Staff Working Document Guidance Document on Listeria monocytogenes Shelf-Life Studies for Ready-to-Eat Foods, under Regulation (EC) No 2073/2005 of 15 November 2005 on Microbiological Criteria for Foodstuffs.* SANCO/11510/2013; European Commission: Brussels, Belgium, 2013.
3. EURL Lm Technical Guidance Document for Conducting Shelf-Life Studies on *Listeria monocytogenes* in Ready-to-Eat Foods. Version 3 of 6 June 2014—Amendment 1 of 21 February 2019. French Agency for Food, Environmental and Occupational Health Safety and European Union Reference Laboratory for *Listeria monocytogenes*. Available online: <https://eurl-listeria.anses.fr/en/system/files/LIS-Cr-201909D2.pdf> (accessed on 23 February 2021).
4. ISO. *Microbiology of the FOOD CHAIN—Requirements and guidelines for Conducting Challenge Tests of Food and Feed Products. Part I: Challenge Tests to Study Growth Potential, Lag Time and Maximum Growth Rate*; ISO 20976-1:2019.E. Switzerland; ISO: Geneva, Switzerland, 2019.
5. Scott, V.N.; Swanson, K.M.; Freier, T.A.; Pruett, W.P., Jr.; Sveum, W.H.; Hall, P.A.; Smoot, L.A.; Brown, D.G. Guidelines for conducting *Listeria monocytogenes* challenge testing of foods. *Food Prot. Trends* **2005**, *25*, 818–825.
6. National Advisory Committee on Microbiological Criteria for Foods. Requisite scientific parameters for establishing the equivalence of alternative methods of pasteurization. *J. Food Prot.* **2006**, *69*, 1190–1216. [[CrossRef](#)] [[PubMed](#)]
7. Zwietering, M.H.; Jongenburger, I.; Rombouts, F.M.; van't Riet, K. Modelling of the bacterial growth curve. *Appl. Environ. Microbiol.* **1990**, *56*, 1875–1881. [[CrossRef](#)] [[PubMed](#)]

8. Baranyi, J.; McClure, P.J.; Sutherland, J.P.; Roberts, T.A. Modeling bacterial growth responses. *J. Ind. Microbiol.* **1993**, *12*, 190–194. [[CrossRef](#)]
9. Buchanan, R.L.; Whiting, R.C.; Damert, W.C. When is simple good enough: A comparison of the Gompertz, Baranyi, and three-phase linear models for fitting bacterial growth curves. *Food Microbiol.* **1997**, *14*, 313–326. [[CrossRef](#)]
10. Huang, L. Optimization of a new mathematical model for bacterial growth. *Food Control* **2013**, *32*, 283–288. [[CrossRef](#)]
11. Ratkowsky, D.A.; Olley, J.; McMeekin, T.A.; Ball, A. Relationship between temperature and growth rate of bacterial cultures. *J. Bacteriol.* **1982**, *149*, 1–5. [[CrossRef](#)] [[PubMed](#)]
12. Juneja, V.K.; Cadavez, V.; Gonzales-Barron, U.; Mukhopadhyay, S. Effect of pH, sodium chloride and sodium pyrophosphate on the thermal resistance of *escherichia coli* O157:H7 in ground beef. *Food Res. Int.* **2015**, *69*, 289–304. [[CrossRef](#)]
13. Juneja, V.; Cadavez, V.; Gonzales-Barron, U.; Mukhopadhyay, S.; Friedman, M. Effect of pomegranate powder on the heat inactivation of *Escherichia coli* O104: H4 in ground chicken. *Food Control* **2016**, *70*, 26–34. [[CrossRef](#)]
14. Gonzales-Barron, U.; Cadavez, V. *Handbook of Predictive Microbiology Growth Models Using R*; Centro de Investigação de Montanha: Bringráfica, Portugal, 2019.
15. Nufer, U.; Stephan, R.; Tasara, T. Growth characteristics of *Listeria monocytogenes*, *Listeria welshimeri* and *Listeria innocua* strains in broth cultures and a sliced bologna-type product at 4 and 7 °C. *Food Microbiol.* **2007**, *24*, 444–451. [[CrossRef](#)] [[PubMed](#)]
16. Pal, A.; Labuza, T.P.; Diez-Gonzalez, F. Evaluating the growth of *Listeria monocytogenes* in refrigerated ready-to-eat frankfurters: Influence of strain, temperature, packaging, lactate and diacetate, and background microflora. *J. Food Prot.* **2008**, *71*, 1806–1816. [[CrossRef](#)] [[PubMed](#)]
17. Lianou, A.; Stopforth, J.D.; Yoon, Y.; Wiedmann, M.; Sofos, J.N. Growth and stress resistance variation in culture broth among *Listeria monocytogenes* strains of various serotypes and origins. *J. Food Prot.* **2006**, *69*, 2640–2647. [[CrossRef](#)] [[PubMed](#)]
18. Aryani, D.C.; Den Besten, H.M.W.; Hazeleger, W.C.; Zwietering, M.H. Quantifying strain variability in modeling growth of *Listeria monocytogenes*. *Int. J. Food Microbiol.* **2015**, *208*, 19–29. [[CrossRef](#)] [[PubMed](#)]
19. R Core Team. *R: A Language and Environment for Statistical Computing*; R Foundation for Statistical Computing: Vienna, Austria, 2013; Available online: <http://www.R-project.org/> (accessed on 23 February 2021).
20. Ross, T. Indices for performance evaluation of predictive models in food microbiology. *J. Appl. Bacteriol.* **1996**, *81*, 501–508. [[PubMed](#)]
21. Pinheiro, J.; Bates, D.; DebRoy, S.; Sarkar, D.; R Core Team. nlme: Linear and Nonlinear Mixed Effects Models. R Package Version 3.1-152. 2021. Available online: <https://CRAN.R-project.org/package=nlme> (accessed on 23 February 2021).
22. ANSES. Development of a Set of *Listeria monocytogenes* Strains for Conducting Challenge Tests. 2013. Available online: <https://sitesv2.anses.fr/en/system/files/private/LIS-Cr-201317R.pdf> (accessed on 23 February 2021).
23. Silva, B.N.; Cadavez, V.; Teixeira, J.A.; Ellouze, M.; Gonzales-Barron, U. Cardinal parameter meta-regression models describing *Listeria monocytogenes* growth in broth. *Food Res. Int.* **2020**, *136*, 109476. [[CrossRef](#)] [[PubMed](#)]
24. COMBASE. A Web Resource for Quantitative and Predictive Food Microbiology. University of Tasmania; USDA Agricultural Research Service. Available online: <https://www.combase.cc/index.php/en/> (accessed on 23 February 2021).
25. Huang, L. Growth kinetics of *Listeria monocytogenes* in broth and beef frankfurters—determination of lag phase duration and exponential growth rate under isothermal conditions. *J. Food Sci.* **2008**, *73*, E235–E242. [[CrossRef](#)] [[PubMed](#)]
26. Liu, Y.; Wang, X.; Liu, B.; Dong, Q. One-Step Analysis for *Listeria monocytogenes* Growth in Ready-to-Eat Braised Beef at Dynamic and Static Conditions. *J. Food Prot.* **2019**, *82*, 1820–1827. [[CrossRef](#)] [[PubMed](#)]
27. Juneja, V.K.; Marks, H.M.; Mohr, T. Predictive Thermal Inactivation Model for Effects of Temperature, Sodium Lactate, NaCl, and Sodium Pyrophosphate on *Salmonella* Serotypes in Ground Beef. *Appl. Environ. Microbiol.* **2003**, *69*, 5138–5156. [[CrossRef](#)] [[PubMed](#)]
28. Juneja, V.; Gonzales-Barron, U.; Butler, F.; Yadav, A.; Friedman, M. Predictive thermal inactivation model for the combined effect of temperature, cinnamaldehyde and carvacrol on starvation-stressed multiple *Salmonella* serotypes in ground chicken. *Int. J. Food Microbiol.* **2013**, *165*, 184–199. [[CrossRef](#)] [[PubMed](#)]